Author Manuscript

Author Manuscript

Author Manuscript

Author Manuscript

HHS Public Access

Author manuscript

*Nat Neurosci*. Author manuscript; available in PMC 2011 March 01.

Published in final edited form as:

*Nat Neurosci*. 2010 September ; 13(9): 1113–1119. doi:10.1038/nn.2616.

# Chronic monoacylglycerol lipase blockade causes functional antagonism of the endocannabinoid system

**Joel E. Schlosburg**[1,†], **Jacqueline L. Blankman**[2,†], **Jonathan Z. Long**[2], **Daniel K. Nomura**[2], **Bin Pan**[4], **Steven G. Kinsey**[1], **Peter T. Nguyen**[1], **Divya Ramesh**[1], **Lamont Booker**[1], **James J. Burston**[1], **Elizabeth A. Thomas**[3], **Dana E. Selley**[1], **Laura J. Sim-Selley**[1], **Qingsong Liu**[4], **Aron H. Lichtman**[1,*], and **Benjamin F. Cravatt**[2,*]

[1]Department of Pharmacology and Toxicology, Virginia Commonwealth University, 410 North 12th Street, Richmond, Virginia 23298, USA

[2]The Skaggs Institute for Chemical Biology and Department of Chemical Physiology, The Scripps Research Institute, 10550 North Torrey Pines Road, La Jolla, California 92037, USA

[3]Department of Molecular Biology, The Scripps Research Institute, 10550 North Torrey Pines Road, La Jolla, California 92037, USA

[4]Department of Pharmacology and Toxicology, Medical College of Wisconsin, Milwaukee, Wisconsin 53226, USA

## Abstract

Prolonged exposure to drugs of abuse, such as cannabinoids and opioids, leads to pharmacological tolerance and receptor desensitization in the nervous system. Here we show that a similar form of functional antagonism is produced by sustained inactivation of monoacylglycerol lipase (MAGL), the principal degradative enzyme for the endocannabinoid 2-arachidonoylglycerol (2-AG). After repeated administration, the MAGL inhibitor JZL184 lost its analgesic activity and produced cross-tolerance to cannabinoid receptor ($CB_1$) agonists in mice, effects that were phenocopied by genetic disruption of MAGL. Chronic MAGL blockade also caused physical dependence, impaired endocannabinoid-dependent synaptic plasticity, and desensitization of brain $CB_1$ receptors. These data contrasted with blockade of fatty acid amide hydrolase (FAAH), an enzyme that degrades the other major endocannabinoid anandamide, which produced sustained analgesia without impairing $CB_1$ receptors. Thus, individual endocannabinoids generate distinct analgesic profiles that are either sustained or transitory and associated with agonism and functional antagonism of the brain cannabinoid system, respectively.

The endogenous cannabinoid (endocannabinoid) system1 consists of two G-protein coupled receptors $CB_1$ and $CB_2$ and their natural lipid ligands *N*-arachidonoylethanolamine (anandamide)2 and 2-arachidonoyglycerol (2-AG)3, 4. The $CB_1$ receptor is highly expressed throughout the nervous system, where it mediates most of the neurobehavioral effects of

Users may view, print, copy, download and text and data- mine the content in such documents, for the purposes of academic research, subject always to the full Conditions of use: http://www.nature.com/authors/editorial_policies/license.html#terms

*To whom correspondence should be addressed: cravatt@scripps.edu, alichtma@vcu.edu.

†These authors contributed equally to the manuscript.

Author Manuscript Author Manuscript Author Manuscript Author Manuscript

cannabinoid agonists, such as $\Delta^9$-tetrahydrocannabinol (THC), the primary psychoactive component of marijuana5. The $CB_2$ receptor is only sparsely expressed in the brain and instead found mainly on immune cells5. . Unlike most other neurotransmitters, which are water-soluble and stored in membrane-delineated vesicles prior to release, the endocannabinoids anandamide and 2-AG are hydrophobic neutral lipids that appear to be biosynthesized and released at the moment of their intended action ("on-demand" production6). These features designate the enzymes involved in endocannabinoid production and degradation as key regulators of signaling7–9. For instance, genetic10, 11 or pharmacological12–15 disruption of fatty acid amide hydrolase (FAAH), the principal degradative enzyme for anandamide16, elevates brain levels of anandamide and produces $CB_1$-dependent analgesia in multiple pain assays. A similar outcome is observed following acute blockade of the 2-AG-degrading enzyme monoacylglycerol lipase (MAGL), which raises 2-AG levels in the nervous system and also reduces pain behavior17, 18. Inhibition of MAGL, however, causes additional behavioral effects not observed following FAAH blockade, including hypomotility and hyperreflexia17, 19, which suggest a broader impact on the brain cannabinoid system. In further support of this premise, MAGL inhibitors, but not FAAH inhibitors, augment depolarization-induced suppression of inhibition (DSI)20 and excitation (DSE)20, 21, forms of synaptic plasticity that have been shown to require the $CB_1$ receptor22 and the 2-AG biosynthetic enzyme diacylglycerol lipase-α23, 24.

The overlapping, but distinct behavioral effects of FAAH and MAGL inhibitors raise provocative questions about the respective roles played by anandamide and 2-AG in the nervous system. Several of the behavioral processes affected by FAAH inhibitors, including pain12–15 and anxiety12, 25, contain a substantial component of stress. In contrast, MAGL inhibitors also appear to impact general neurological functions (e.g., locomotor activity)17, 19. Could these pharmacological profiles point to a broader role for 2-AG in the nervous system, with anandamide functioning as a more restricted, stress-responsive endocannabinoid? If so, what might be impact of sustained elevations in anandamide and 2-AG on the integrity of the endocannabinoid system?

Here, we show that prolonged pharmacological or genetic inactivation of MAGL causes profound alterations in the brain endocannabinoid system in mice, as evidenced by a loss of analgesic responses to a MAGL inhibitor, cross-tolerance to exogenous cannabinoid agonists, and $CB_1$ receptor downregulation and desensitization in specific brain regions. In contrast, none of these effects were observed in animals with chronically disrupted FAAH, which instead maintained an analgesic phenotype and intact $CB_1$ receptor system. These findings thus point to fundamental differences in the mode of signaling for two major endocannabinoid pathways in the nervous system that result in either sustained agonism or functional antagonism. That these effects occur through the same receptor ($CB_1$) implicates ligand diversification as a major mechanism by which the endocannabinoid system modulates mammalian physiology and behavior.

Author Manuscript Author Manuscript Author Manuscript Author Manuscript

## Results

### Mouse models for chronic inactivation of MAGL

We established complementary pharmacological and genetic models to examine the consequences of sustained elevations in 2-AG in the nervous system. We generated a chronic pharmacological model by treating mice for six consecutive days with the MAGL inhibitor JZL184 (40 mg/kg, i.p., once per day dosing), which has previously been shown to selectively inactivate MAGL in the nervous system and raise brain 2-AG by up to 10-fold over control levels17. Mice treated with JZL184 acutely (single dose) or chronically showed highly elevated brain levels of 2-AG two hours following final dosing (Fig. 1a). This increase in brain 2-AG levels persisted for at least 26 h (Supplementary Fig. 1), indicating that 2-AG remained elevated throughout the repeated dosing regime. Chronic, but not acute, dosing also caused a modest elevation in anandamide (~three-fold) two hours after final treatment (Fig. 1a), likely reflecting a partial blockade of FAAH17 as a result of cumulative exposure to JZL184 over the treatment regimen. This change was, however, much lower than the 15-fold rise in brain anandamide observed in mice treated for one or six days with the selective FAAH inhibitor PF-384515 (10 mg/kg, i.p., once per day dosing; Fig. 1a) and was not of prolonged duration (Supplementary Fig. 1). PF-3845 did not alter brain 2-AG levels after acute or chronic treatment (Fig. 1a).

We also employed *MAGL*$^{-/-}$ mice as a complementary genetic model for sustained elevations in 2-AG. We obtained *MAGL*$^{-/-}$ mice generated by gene trapping from the Texas A&M Institute for Genomic Medicine (Fig. 1b,c), and confirmed by activity-based protein profiling26,27 that these animals lack detectable MAGL activity without showing alterations in other brain serine hydrolase activities, including FAAH (Fig. 1d and Supplementary Fig. 2a). We also confirmed the absence of MAGL expression in *MAGL*$^{-/-}$ mice by *in situ* hybridization and mass spectrometry-based proteomics (Supplementary Fig. 3). *MAGL*$^{-/-}$ mice exhibited dramatic (~90%) reductions in brain 2-AG hydrolytic activity (Fig. 1e and Supplementary Fig. 2b) and ~10-fold elevations in brain 2-AG levels (Fig. 1f and Supplementary Table 1). Brain arachidonic acid levels were also significantly reduced in *MAGL*$^{-/-}$ mice (Fig. 1f and Supplementary Table 1) or mice treated acutely or chronically with JZL184 (Supplementary Fig. 2c), consistent with previous findings designating 2-AG as a physiological precursor for arachidonic acid in the brain17, 28. Anandamide levels were unaltered in *MAGL*$^{-/-}$ mice (Fig. 1f and Supplementary Table 1). We observed similar metabolic changes in a panel of peripheral tissues from JZL184-treated29 or *MAGL*$^{-/-}$ mice, all of which showed significant reductions in 2-AG hydrolysis and elevations in 2-AG, but not anandamide (Supplementary Fig. 4). These data provide genetic confirmation that MAGL is the principal 2-AG hydrolase in the mouse brain and many peripheral tissues and establish *MAGL*$^{-/-}$ mice as a valid animal model to probe the neurophysiological and behavioral consequences of sustained elevations in 2-AG.

### Chronic MAGL blockade causes tolerance in pain assays

Acute pharmacological blockade of MAGL or FAAH produced similar efficacy in multiple pain assays, including antinociception in the acute thermal tail withdrawal test (Fig. 2a) and reductions in mechanical (Fig. 2b) and cold (Fig. 2c) allodynia in the chronic constrictive

Author Manuscript Author Manuscript Author Manuscript Author Manuscript

injury of the sciatic nerve (CCI) model. In contrast, prolonged disruption of these enzymes resulted in a striking difference in the expression of tolerance. Whereas mice treated repeatedly with PF-3845 maintained hypoalgesic (Fig. 2a) and anti-allodynic (Fig. 2b,c) responses, mice chronically treated with JZL184 showed similar pain responses as control mice (Fig. 2a–c). Likewise, *MAGL*$^{-/-}$ mice displayed equivalent tail withdrawal latencies as *MAGL*$^{+/+}$ and *MAGL*$^{+/-}$ mice. (Fig. 2d).

These findings indicate that the analgesic effects produced by acute blockade of MAGL are lost following sustained inactivation of this enzyme. We next investigated whether this form of tolerance was due to alterations in the endocannabinoid system.

## Chronic MAGL blockade causes tolerance to CB1 agonists

We assessed the behavioral effects of cannabinoid receptor agonists in animals with chronic disruptions in FAAH or MAGL. *FAAH*$^{-/-}$ mice10, as well as mice treated chronically with PF-3845 (Supplementary Fig. 5) exhibit wild-type responses to cannabinoids in antinociception, hypothermia, and catalepsy assays, indicating normal $CB_1$ function in these animals. In contrast, *MAGL*$^{-/-}$ mice or mice treated chronically with JZL184 showed significantly reduced responses to the antinociceptive and hypothermic effects of THC (Supplementary Fig. 6) or the full $CB_1$ agonist WIN55,212-2 (Fig. 3). Chronic JZL184 treatment also elicited marked cross-tolerance to the anti-allodynic effects of WIN55,212-2 or PF-3845 in the CCI model (Fig. 2e,f). $CB_1$ agonist-induced catalepsy was less affected by sustained inactivation of MAGL (Fig. 3c,f and Supplementary Fig. 6). These data indicate that sustained inactivation of MAGL causes cross-tolerance to exogenous $CB_1$ agonists, as well as to a FAAH inhibitor in a neuropathic pain model.

We next asked whether prolonged MAGL or FAAH blockade produces physical dependence, a phenotype that has been observed in rodents exposed to repeated treatments with direct $CB_1$ agonists30.. The CB1 receptor antagonist rimonabant precipitated paw flutters in mice treated chronically with JZL184 to a similar degree as mice treated with a mild THC chronic dosing regimen (10 mg/kg per day for six days) (Supplementary Fig. 7). In contrast, rimonabant did not precipitate paw tremors in mice chronically administered PF-3845.

## Brain $CB_1$ receptors are impaired by chronic MAGL blockade

The loss of analgesic responses and occurrence of cannabinoid cross-tolerance in mice with sustained disruptions of MAGL suggested that $CB_1$ receptors might be downregulated and/or desensitized in these animals. In support of this hypothesis, brain tissue from *MAGL*$^{-/-}$ mice or mice chronically treated with JZL184 showed significant decreases in $CB_1$ receptor number and function as measured through specific binding of $^3$H-rimonbabant and $CB_1$ agonist (CP55,940)-stimulated [$^{35}$S]-GTPγS binding, respectively (Fig. 4a,b; Supplementary Fig. 8 and **Supplementary Table 2**). In contrast, prolonged blockade of FAAH by PF-3845 did not impact $CB_1$ receptor expression or function (Fig. 4a,b; Supplementary Fig. 8 and **Supplementary Table 2**). These findings are consistent with previous work showing no loss of $CB_1$ receptor number or function in *FAAH*$^{-/-}$ mice31, 32.

Author Manuscript Author Manuscript Author Manuscript Author Manuscript

To provide further evidence that the behavioral tolerance and $CB_1$ receptor adaptations caused by chronic MAGL blockade were due to elevated 2-AG acting on $CB_1$ receptors (as opposed to other metabolic alterations, such as reductions in arachidonic acid), we attempted to block these changes by concurrent chronic treatment with rimonabant. For technical reasons, we focused on antinociception for our behavioral measurements (see Supplementary Discussion). Over a six day period, we treated mice daily with vehicle, JZL184 (40 mg/kg, i.p.), rimonabant (3 mg/kg, i.p.), or both JZL184 (40 mg/kg, i.p.) and rimonabant (3 mg/kg) to give four treatment groups. As shown previously (Fig. 3), chronic JZL184-treated mice produced marked tolerance to the anti-nociceptive effects of WIN55,212-2 (Supplementary Fig. 9a). In contrast, the rimonabant-JZL184-treated animals exhibited significantly greater antinociceptive responses to WIN55,212-2 that were close in magnitude to those observed in control (vehicle or rimonabant) animals (Supplementary Fig. 9a). These data indicate that daily treatment with rimonabant substantially prevents the nociceptive adaptations caused by chronic MAGL blockade. Rimonabant treatment (10 mg/kg, i.p.) also ameliorated brain $CB_1$ receptor adaptations in chronic JZL184-treated animals mice as judged by CP55,940-stimulated [$^{35}$S]-GTPγS binding (Supplementary Fig. 9b,c).

A more extensive regional analysis of CP55,940-stimulated [$^{35}$S]GTPγS binding in mice treated chronically with either vehicle or JZL184 revealed that chronic MAGL blockade produced a hetergoenous reduction in CB1 function throughout the brain (Fig. 5). Notable brain regions showing significant $CB_1$ desensitization include the cingulate cortex, hippocampus, somatosensory cortex, and PAG (Fig. 5b). In contrast, chronic JZL184 treatment did not elicit desensitization in the caudate putamen or globus pallidus.

These data, taken together, indicate that prolonged inactivation of MAGL, but not FAAH causes marked changes in $CB_1$ receptor expression and function in specific brain regions, including those that participate in pain perception (e.g., the PAG) and cognitive/emotional processing of pain33 (e.g., cingulate cortex).

## Synaptic plasticity is impaired by chronic MAGL blockade

Endocannabinoids regulate several forms of synaptic plasticity34, including DSI in the hippocampus20. Considering that $CB_1$ receptors were significantly altered in this brain region by sustained MAGL inactivation, we asked whether DSI was also affected. In contrast to previous research demonstrating that acute inhibition of MAGL by bath application of JZL184 potentiates DSI in mouse hippocampal slices20, we observed significant decreases in the magnitude and time constant (τ) of DSI in hippocampal slices from mice treated chronically with JZL184 when compared to slices from vehicle-treated mice (Fig. 6a). We observed similar effects in layer V pyramidal neurons of the cingulate cortex, where acute (Supplementary Fig. 10) and chronic (Fig. 6b) treatment with JZL184 potentiated and disrupted DSI, respectively. PF-3845 did not affect DSI in the hippocampus (Fig. 6a) or cingulate cortex (Fig. 6b and Supplementary Fig. 10).

The attenuation of DSI by chronic JZL184 treatment is consistent with desensitization of $CB_1$ receptors in the affected neuronal circuits (Fig. 5). In support of this premise, CP55,940 (3 μM) induced significantly less depression of inhibitory postsynaptic currents (IPSCs) in

Author Manuscript Author Manuscript Author Manuscript Author Manuscript

hippocampal CA1 pyramidal neurons or layer V pyramidal neurons of the cingulate cortex from chronically JZL184-treated mice compared to vehicle-treated mice (Fig. 6c,d). In contrast, repeated *in vivo* administration of PF-3845 did not significantly alter CP55,940-induced depression of IPSCs in either hippocampus (Fig. 6c) or cingulate cortex (Fig. 6d). The $CB_1$ receptor antagonist AM251 (2 μM) completely blocked CP55,940-induced depression of IPSCs in both brain regions (Supplementary Fig. 11). Interestingly, chronic JZL184 treatment exerted only a modest effect that did not reach statistical significance on CP55,940-induced depression of IPSCs in the caudate putamen (Supplementary Fig. 12), a brain region that also showed minimal $CB_1$ receptor adaptations (Fig. 5).

Recent studies suggest that $CB_1$ receptors on glutamatergic synapses mediate many of the behavioral effects of $CB_1$ agonists35. We therefore examined whether chronic JZL184 or PF-3845 treatment altered $CB_1$-mediated depression of glutamatergic excitatory transmission in the hippocampus. Chronic JZL184, but not PF-3845 treatment significantly attenuated CP55,940-induced depression of field excitatory postsynaptic potentials (fEPSPs) in the CA1 region of the hippocampus (Supplementary Fig. 13).

These results, taken together, demonstrate that sustained inactivation of MAGL, but not FAAH, significantly attenuates specific endocannabinoid-mediated forms of synaptic plasticity. That we observed these effects for both glutamatergic and GABAergic transmission is consistent with previous research showing that acute MAGL, but not FAAH blockade enhances both DSE and DSI20, and recent studies demonstrating that diacylglycerol lipase-$\alpha^{-/-}$ mice exhibit defects in both DSE and DSI23, 24.

## Discussion

Prolonged treatment with THC and other cannabinoid receptor agonists leads to the development of tolerance and physical dependence36, and these behavioral phenotypes have been shown to be mirrored by substantial reductions in $CB_1$ receptor expression and activity in the brain37, 38. In this study, we found that sustained elevations in brain 2-AG caused by either genetic deletion or chronic pharmacological blockade of MAGL also produces substantial functional antagonism of the brain endocannabinoid system, as manifested by tolerance to the analgesic effects of acute enzyme inhibition, cross-tolerance to $CB_1$ receptor agonists, a reduction in $CB_1$ receptor expression and function, and disruptions in endocannabinoid-dependent synaptic plasticity. This profile markedly contrasted with that of sustained pharmacological disruption of FAAH, which caused persistent analgesic effects without evidence of tolerance or changes in $CB_1$ receptor expression or function. Thus, brain $CB_1$ receptors undergo markedly different adaptations in response to sustained elevations of the two principal endocannabinoids, 2-AG and anandamide.

That the cannabinoid cross-tolerance and alterations in $CB_1$ receptor function caused by JZL184 were both attenuated by co-treatment rimonabant supports a model where chronic MAGL blockade produces a sustained elevation in 2-AG that tonically activates, and eventually desensitizes $CB_1$ receptors in the brain. We cannot, however, rule out the possibility that other metabolic changes caused by MAGL inhibition, such as reductions in arachidonic acid, also contribute to alterations in brain endocannabinoid pathways. We also

Author Manuscript Author Manuscript Author Manuscript Author Manuscript

note that chronic JZL184 treatment produced an evidently larger degree of cross-tolerance to $CB_1$ agonists (Fig. 3a,b) than genetic disruption of MAGL (Fig. 3d,e). Although we do not yet understand the basis for this difference, it could reflect differences in background strain (C57BL/6J versus 129SvEv/C57BL/6J for the JZL184-treated and *MAGL*$^{-/-}$ mice, respectively) or the existence of compensatory mechanisms in the *MAGL*$^{-/-}$ mice that counteract the observed $CB_1$ receptor adaptations.

Although there are other examples of functional antagonism of receptor systems following deletion of a metabolic enzyme, including reduced activity of nicotinic receptors39 in acetylcholinesterase$^{-/-}$ mice and impairments in 5-HT1A receptors in monoamine oxidase A$^{-/-}$ mice40, we report the first instance, to our knowledge, where disruption of an enzyme that degrades a lipid transmitter led to receptor downregulation and desensitization in the nervous system. This intriguing finding indicates that, despite fundamental differences in mechanism of storage and release (vesicular versus non-vesicular), classical neurotransmitters and lipid messengers are both capable of causing tolerance and receptor desensitization following chronic inactivation of their cognate degradative enzymes. That behavioral and $CB_1$ receptor adaptations occurred only in mice with chronically inactivated MAGL, but not FAAH, indicates that sustained elevations in 2-AG exert a greater impact than anandamide on the integrity of the brain endocannabinoid system. How 2-AG is more capable of causing substantial CB1 alterations *in vivo* remains unclear, but our data would indicate that this effect is not necessarily correlated with the induction of superior efficacy in behavioral assays. Indeed, MAGL and FAAH inhibitors displayed similar relative analgesic activity in acute treatment paradigms. One possibility is that 2-AG and anandamide exert differential impact on $CB_1$ receptor desensitization and/or recycling in the brain, as has been observed previously in heterologous expression systems41. This differential desensitization may be related to the higher efficacy that 2-AG displays as a full $CB_1$ receptor agonist (in contrast to anandamide, which acts as a partial $CB_1$ receptor agonist)42, though previous research suggests that the magnitude of $CB_1$ receptor desensitization is not related to the intrinsic activity of exogenous agonists43. Bulk brain levels of 2-AG are also much higher than anandamide (see Fig. 1a) (although the interstitial levels of these endocannabinoid are similar44), and therefore elevated 2-AG may achieve greater occupancy of $CB_1$ receptors *in vivo*. Finally, MAGL and FAAH are found in different neuronal populations and subcellular compartments (pre- and postsynaptic, respectively) throughout the brain, and these anatomical distinctions might also differentially affect endocannabinoid signaling pathways in the nervous system. Regardless, our observation that chronic MAGL blockade produced cross-tolerance to a FAAH inhibitor in the CCI model (Fig. 2e,f) indicates that 2-AG and anandamide pathways can crosstalk in the neural circuits that regulate pain behavior.

The endocannabinoid system regulates several forms of synaptic plasticity, including DSI and DSE34. Acute MAGL, but not FAAH inhibition potentiates DSI in neurons of the hippocampus20 and cingulate cortex (Supplementary Fig. 4). Strikingly, however, we found that repeated administration of JZL184 led to profound DSI deficits in these neuronal populations (Fig. 6). These impairments in short-term synaptic plasticity are consistent with the observed alterations in $CB_1$ receptor function in the hippocampus and cingulate cortex (Fig. 5), as deletion or antagonism of this receptor has been shown to abolish DSI22, 45.

Author Manuscript Author Manuscript Author Manuscript Author Manuscript

That acute and chronic inhibition of MAGL produced opposing effects on DSI in multiple brain regions supports a model in which prolonged elevations of endogenous 2-AG cause functional antagonism of $CB_1$ receptors in the nervous system.

In contrast to direct $CB_1$ agonists, which produce cross-tolerance to the antinociceptive, hypothermic, and cataleptic effects of THC and WIN55,212-246, chronic MAGL disruption only caused strong cross-tolerance to the antinociceptive and hypothermic effects of these drugs. The minimal cross-tolerance to cannabinoid-induced catalepsy is consistent with the lack of $CB_1$ receptor desensitization in caudate putamen and globus pallidus (Fig. 5), which are associated with cannabinoid-induced catalepsy47. Conversely, the tolerance we observed to the antinociceptive effects of JZL184 and the occurrence of cross-tolerance to WIN55,212-2 and THC-induced antinociception could be attributed to the significant desensitization of $CB_1$ receptors in PAG (Fig. 5), a brain area strongly implicated in cannabinoid-induced antinociception48. We also note that neither MAGL nor FAAH inhibitors, on their own, cause catalepsy; however, combined treatment with these inhibitors does promote cataleptic behavioral responses19. It will be interesting in future studies to determine whether sustained inactivation of both MAGL and FAAH causes cross-tolerance to the cataleptic effects of other $CB_1$ agonists and concomitant alterations in $CB_1$ receptor expression and activity in brain regions such as the caudate putamen and globus pallidus.

In summary, our data support a model where ligand diversification plays a major role in shaping the distinct functions and properties of endocannabinoid signaling pathways in the nervous system. The widespread behavioral and $CB_1$ receptor adaptations caused by chronic disruption of MAGL point to a broad role for 2-AG throughout the nervous system. In contrast, the preservation of analgesic phenotypes and $CB_1$ receptor function in mice with sustained inactivation of FAAH may reflect a more limited, stress-dependent function for anandamide. This idea is also consistent with the behavioral phenotypes observed in FAAH-disrupted animals, which preferentially show reductions in pain11 and anxiety25 paradigms with strong stress components. These discoveries may have important translational implications. Consider, for instance, that acute inhibition of FAAH and MAGL produces similar efficacy in multiple pain assays, but these effects are only sustained in chronically disrupted FAAH systems. Might this imply that MAGL is a less suitable target for treatment of pain disorders? Perhaps, but it also may be possible to achieve prolonged analgesic responses through partial MAGL blockade. In this event, one would still need to be concerned about the potential tolerance and withdrawal effects of MAGL inhibitors. That $CB_1$ receptors, on the other hand, are surprisingly non-adaptive to continuous elevations of brain anandamide suggests that FAAH inhibitors are capable of producing sustained analgesic activity without high risk for dependence.

## Methods

### Subjects

Subjects consisted of male C57BL/6J mice (Jackson Laboratories; Bar Harbor, ME) as well as male and female *MAGL*$^{+/+}$, *MAGL*$^{+/-}$, and *MAGL*$^{-/-}$ mice on a mixed 129SvEv/C57BL/6J background. *Mgll*$^{Gt1(neo)}$ mutant mice (TG0078; derived from OmniBank® ES cell line OST113734) containing a gene trap vector inserted into the third intron of the *Mgll*

Author Manuscript Author Manuscript Author Manuscript Author Manuscript

gene were obtained from the Texas Institute of Genomic Medicine (TIGM). The gene trap vector insertion site (denoted by *) was mapped to the sequence GCCTTGTGGACTGGAT*CTTGGGCCTTCTGTTC, which is upstream of the *Mgll* catalytic exon 4. MAGL genotype was determined by PCR amplification of genomic tail DNA using the following primers designed by TIGM: *Mgll* forward 5'-TTGCCTGCTTGCTCTTAACTCTTGC-3', *Mgll* reverse 5'-GGGAGTCAAGACACTGGGGAATCCT-3', and gene trap reverse 5'-ATAAACCCTCTTGCAGTTGCATC-3', which amplified a 430 bp product for the wild-type allele and a 220 bp product for the gene-trapped allele. Mice homozygous for the gene-trap ($MAGL^{-/-}$ mice) are viable, born at the expected Mendelian frequency, and display normal cage behavior compared with $MAGL^{+/+}$ and $MAGL^{-/-}$ littermates. Animal experiments were conducted in accordance with the guidelines of the Institutional Animal Care and Use Committees of The Scripps Research Institute and Virginia Commonwealth University

## Drugs and Chemicals

JZL184 and PF-3845 were synthesized as described previously15, 17. WIN55,212 was purchased from Cayman Chemical (Ann Arbor, MI). Rimonabant, $\Delta^9$-THC, and CP55,940 were obtained from the Drug Supply Program of the National Institute on Drug Abuse (Rockville, MD). AM251 was obtained from Tocris (Ellisville, MO). GDP, GTPγS, adenosine deaminase, and bovine serum albumin (BSA) were purchased from Sigma-Aldrich (St. Louis, MO). [$^{35}$S]GTPγS (1250 Ci/mmol) was obtained from PerkinElmer Life and Analytical Sciences (Waltham, MA). [$^{3}$H]SR141716A (44.0 Ci/mmol) was purchased from Amersham Pharmacia (Piscataway, NJ). Scintillation fluid (ScinitSafe Econo 1) was purchased from Thermo Fisher Scientific (Waltham, MA) and Whatman GF/B glass fiber filters (Whatman, Clifton, NJ) were obtained through Fisher Scientific (Pittsburgh, PA).

Drugs were dissolved via sonification in a vehicle consisting of ethanol, Alkamuls-620 (Sanofi-Aventis, Bridgewater, NJ), and saline in a ratio of 1:1:18. All drugs were administered via the i.p. route of administration in a volume of 10 μL/g body mass. For chronic drug administration, subjects received a daily injection of JZL184 (40 mg/kg), PF-3845 (10 mg/kg), THC (10 mg/kg), rimonabant (3 mg/kg for behavioral analysis, 10 mg/kg for $CB_1$ receptor adaptation), or vehicle for six days.

## Preparation of mouse brain homogenates

Membrane and soluble brain homogenates from C57BL6/J and $MAGL^{+/+}$, $MAGL^{+/-}$, and $MAGL^{-/-}$ mice (n = 4 per genotype) were prepared as previously described29.

## Activity-based protein profiling (ABPP) analysis

ABPP analysis of brain proteomes pre-treated with 5 μM JZL184 or DMSO vehicle (30 min at 25°C) was performed as described previously27.

Author Manuscript Author Manuscript Author Manuscript Author Manuscript

### 2-AG hydrolysis assays

2-AG hydrolytic activity of *MAGL*$^{+/+}$, *MAGL*$^{+/-}$, and *MAGL*$^{-/-}$ brain homogenates (n = 4 per genotype) pretreated with either 1 μM JZL184 or DMSO vehicle (30 min at 25°C) was determined using a previously described LC-MS assay27 on an Agilent 6520 QTOF MS.

### Brain metabolite measurements

Brain lipid levels were determined as previously described29 except that FFA levels in *MAGL*$^{+/+}$, *MAGL*$^{+/-}$, and *MAGL*$^{-/-}$ brains were measured on an Agilent 1100 series LC-MS and quantified compared to a palmitic acid calibration curve.

### *In situ* hybridization

Perfused brains from 12 week old male *MAGL*$^{+/+}$ and *MAGL*$^{-/-}$ mice were postfixed, cryoprotected and frozen as previously described49. *In situ* hybridization was performed on 25-μm thick free-floating coronal sections as described49 with [$^{35}$S]UTP-labeled, single-stranded antisense and sense control cRNA probes against MAGL cDNA bases 285–600.

### Multidimensional LC-MS proteomic analysis

Mouse brain proteomes (0.75 mg total protein) from *MAGL*$^{+/+}$ and *MAGL*$^{-/-}$ mice (n = 3 mice per genotype) were precipitated with 1:4 chloroform:methanol and denatured with 25 mM ammonium bicarbonate in 6 M urea. Samples were reduced with 10 mM dithiothreitol, alkylated with 40 mM iodoacetamide, and diluted to 2 M urea with 25 mM ammonium bicarbonate. Digestion with trypsin (0.5 μg/μL) was performed overnight at 37°C in the presence of 1 mM $CaCl_2$. The tryptic peptide samples were acidified with 5% formic acid and aliquots were frozen at −80°C until use. Multidimensional protein identification technology (MudPIT) analysis was performed as previously described27 on an LTQ mass spectrometer (ThermoFinnigan) coupled to an Agilent 1100 series HPLC (n = 2 per genotype, 30 μg protein, 5-step MudPIT) or an LTQ Orbitrap Velos mass spectrometer (ThermoFinnigan) coupled to an Agilent 1200 series HPLC (n = 1 per genotype, 45 μg protein, 10-step MudPIT). The tandem MS data were searched against the mouse IPI database using the SEQUEST search algorithm, and results were filtered and grouped with DTASELECT. Peptides with cross-correlation scores greater than 1.8 (+1), 2.5 (+2), 3.5 (+3) and delta CN scores greater than 0.08 were included in the spectral counting analysis.

### Behavioral assays

To control for stress of repeated injection, all acute treatment groups received 5 days of daily vehicle injections, with acute drug treatment occurring on day 6. Subjects were evaluated 2 h after acute drug administration or the final chronic injection. Acute thermal antinociception was assessed in the tail immersion test at 56.0°C using a 10 s cut-off19. Surgery for chronic constriction injury (CCI) model of the sciatic nerve and allodynia assessment were performed as previously described18. Subjects were assessed for mechanical allodynia using von Frey filaments (North Coast Medical, Morgan Hill, CA) and approximately 30 min later were evaluated for cold allodynia in the acetone-induced paw lifting model, with a maximum cutoff time of 20 s. Cross-tolerance studies in the CCI model were performed starting 26 h following the final chronic drug injection.

Author Manuscript Author Manuscript Author Manuscript Author Manuscript

Twenty-six or 48 h after the final chronic injection, subjects were evaluated for cross-tolerance to WIN55,212-2 or THC. Cannabimimetic activity was assessed by evaluating mice for catalepsy in the bar test19, antinociception in the tail immersion test at 52.0 °C31, and hypothermia by inserting a thermocouple probe 2.0 cm into the rectum. In order to reduce the number of mice required for this study, dose-response relationships were evaluated using a cumulative dosing regimen in which baseline behavioral endpoints were assessed, injections were given every 40 min, and subjects were evaluated for each measure 30 min after each injection, with the entire dose-response assessment completed in less than 4 h31.

For precipitated withdrawal, animals were challenged with rimonabant (10 mg/kg) 2 h after the final chronic injection, and the incidents of paw fluttering, including any tremors or shaking of the front paws, were recorded for a 1 h observation period50.

## Binding Assays

CP-55,940-stimulated [$^{35}$S]GTPγS binding and [$^{3}$H]-SR141716A binding in whole brains were conducted as previously described31. For CP-55,940-stimulated [$^{35}$S]GTPγS autoradiographs, coronal sections (20 μm) were cut on a cryostat at −20°C, thaw-mounted onto gelatin-subbed slides, and stored desiccated at −80°C until use. For assay, slides were brought to room temperature, incubated in Assay Buffer + 0.5% BSA containing 0.04 nM [$^{35}$S]GTPγS in the presence or absence (basal) of maximally effective concentrations of CP55,940 (3 μM) and/or vehicle for 2 h at 25°C. After final incubation, slides were rinsed twice in 50 mM Tris buffer (pH 7.4) at 4°C and then rinsed in deionized water. The rinsed slides were dried, and exposed to Kodak BioMax MR film with [$^{14}$C] standards for 24–36 h. Films were digitized at 8-bits per pixel with a Sony XC-77 video camera. Regions of interest were selected using anatomical landmarks and measured using NIH ImageJ software.

## Electrophysiology slice preparation and testing

In the chronic experiments, subjects were anaesthetized by isoflurane inhalation and decapitated 24–26 h after the final injection. Hippocampal slices and cortical slices (300 μm thick) were cut using a vibrating slicer (Leica) and prepared, as described previously20. In the acute experiments, the slices were perfused with JZL184 (1 μM) or PF-3845 (10 μM) for 40–80 min.

Whole-cell voltage-clamp recordings were made using patch clamp amplifier (Multiclamp 700B) under infrared-DIC microscopy. Data acquisition and analysis were performed using a digitizer (DigiData 1440A) and analysis software pClamp 10 (Molecular Devices). To record IPSCs, the neurons were clamped at −60 mV, and the pipettes were filled with an internal solution containing (in mM): 80 Cs-methanesulfonate, 60 CsCl, 5 QX-314, 10 HEPES, 0.2 EGTA, 2 $MgCl_2$, 4 MgATP, 0.3 $Na_2$GTP, and 10 $Na_2$-phosphocreatine (pH 7.2 with CsOH). Glutamate receptor antagonists 6-cyano-7-nitroquinoxaline-2,3-dione (CNQX, 20 μM) and D-2-amino-5-phosphonovaleric acid (D-AP-5, 25 μM) were present in the ACSF throughout the experiments. Series resistance (15–30 MΩ) was monitored throughout the recordings, and data were discarded if the resistance changed by more than 20%. To record fEPSPs, the pipettes were filled with 1 M NaCl, and picrotoxin (50 μM) was present

Author Manuscript Author Manuscript Author Manuscript Author Manuscript

in the ACSF. To evoke IPSCs or fEPSPs, a bipolar tungsten stimulation electrode was placed in the in the stratum radiatum of the CA1 region of hippocampus, in layer V of cingulate cortex or the CPu. All recordings were performed at 32 ± 1°C by using an automatic temperature controller.

### Data analysis and statistics

All results are expressed as mean ± s.e.m. unless otherwise noted. Results were considered to be significant at $p < 0.05$. All lipid quantification and behavioral endpoints were initially evaluated by ANOVA (treatment or genotype), or repeated measures ANOVA (cumulative dose-responses). Following a significant ANOVA Dunnett's post hoc test was performed for comparisons to treatment or genotypic control. Planned comparisons and specific within-drug treatments are noted in figure captions when used, using a Bonferroni test to correct for multiple comparisons. [$^{35}$S]GTPγS binding experiments were performed in triplicate, and all data points are reported as mean ± SEM of four experiments. Nonspecific binding was first subtracted from all binding data. Stimulated binding was determined as agonist-stimulated binding minus basal binding, and values are reported as percentage stimulation above basal. All receptor binding experiments were performed in duplicate and reported as mean ± SEM of four experiments. Nonspecific binding was first subtracted from total binding, yielding specific binding data. Nonlinear regression analyses of agonist concentration-effect curves were performed with Prism 5.0 using a sigmoidal dose-response model or specific binding of single site model (GraphPad Software Inc., San Diego, CA). Values reported from regressions as mean ± SEM for interpolated results. Regional G-protein stimulation autoradiography data are reported as mean ± SEM of triplicate sections from 7–8 brains/group. Net [$^{35}$S]GTPγS binding is defined as (agonist-stimulated [$^{35}$S]GTPγS binding – basal [$^{35}$S]GTPγS binding). Analysis was performed in GraphPad Prism Version 5 using Student's *t*-test between the two treatments for each individual region analyzed. For electrophysiological analysis, IPSC amplitude was normalized to the baseline. The decay time constant (τ) of DSI was measured using a single exponential function of $y = y_0 + k \times \exp(-x/\tau)$. The magnitude of DSI was calculated as follows: DSI (%) = 100 × [1- (mean amplitude of 2 IPSCs immediately after depolarization/mean amplitude of 5 IPSCs before depolarization)]. Values of 2–3 DSI trials were averaged for each neuron. The depression (%) of IPSCs/fEPSPs by CP55,940 was calculated as follows: 100 × [mean amplitude of IPSCs/fEPSPs during the last 5 min treatment/mean amplitude of baseline IPSCs/fEPSPs]. Data sets were compared with Student's *t*-test.

## Supplementary Material

Refer to Web version on PubMed Central for supplementary material.

## Acknowledgements

We thank S. Niessen and H. Hoover for assistance with proteomics studies, I. Beletskaya and R. Abdullah for technical support and the Cravatt and Lichtman labs for critical reading of the manuscript. This work was supported by the National Institutes of Health (DA017259, DA009789, DA025285, DA005274, DA015683, DA03672, DA005274, DA07027, DA014277, DA023758, DA024741), Ruth L. Kirschstein NIH Predoctoral Fellowships [DA026261 (JLB), DA026279 (JES), DA028333 (LB), DA023758 (PTN)], the American Cancer Society (DKN), and the Skaggs Institute for Chemical Biology.

Author Manuscript Author Manuscript Author Manuscript Author Manuscript

## References


1. Pacher P, Bátkai S, Kunos G. The Endocannabinoid System as an Emerging Target of Pharmacotherapy. Pharmacol. Rev. 2006; 58:389–462. [PubMed: 16968947]
2. Devane WA, et al. Isolation and structure of a brain constituent that binds to the cannabinoid receptor. Science. 1992; 258:1946–1949. [PubMed: 1470919]
3. Mechoulam R, et al. Identification of an endogenous 2-monoglyceride, present in canine gut, that binds cannabinoid receptors. Biochem. Pharmacol. 1995; 50:83–90. [PubMed: 7605349]
4. Sugiura T, et al. 2-Arachidonylglycerol: a possible endogenous cannabinoid receptor ligand in brain. Biochem. Biophys. Res. Commun. 1995; 215:89–97. [PubMed: 7575630]
5. Mackie K. Cannabinoid receptors as therapeutic targets. Annu Rev Pharmacol Toxicol. 2006; 46:101–122. [PubMed: 16402900]
6. Marsicano G, et al. CB1 cannabinoid receptors and on-demand defense against excitotoxicity. Science. 2003; 302:84–88. [PubMed: 14526074]
7. Fowler CJ. The cannabinoid system and its pharmacological manipulation--a review, with emphasis upon the uptake and hydrolysis of anandamide. Fundam Clin Pharmacol. 2006; 20:549–562. [PubMed: 17109648]
8. Ahn K, McKinney MK, Cravatt BF. Enzymatic pathways that regulate endocannabinoid signaling in the nervous system. Chem Rev. 2008; 108:1687–1707. [PubMed: 18429637]
9. Deutsch DG, Chin SA. Enzymatic synthesis and degradation of anandamide, a cannabinoid receptor agonist. Biochem Pharmacol. 1993; 46:791–796. [PubMed: 8373432]
10. Cravatt BF, et al. Supersensitivity to anandamide and enhanced endogenous cannabinoid signaling in mice lacking fatty acid amide hydrolase. Proc. Natl. Acad. Sci. U.S.A. 2001; 98:9371–9376. [PubMed: 11470906]
11. Lichtman AH, Shelton CC, Advani T, Cravatt BF. Mice lacking fatty acid amide hydrolase exhibit a cannabinoid receptor-mediated phenotypic hypoalgesia. Pain. 2004; 109:319–327. [PubMed: 15157693]
12. Kathuria S, et al. Modulation of anxiety through blockade of anandamide hydrolysis. Nat Med. 2003; 9:76–81. [PubMed: 12461523]
13. Lichtman AH, et al. Reversible inhibitors of fatty acid amide hydrolase that promote analgesia: evidence for an unprecedented combination of potency and selectivity. J Pharmacol Exp Ther. 2004; 311:441–448. [PubMed: 15229230]
14. Jhaveri MD, Richardson D, Kendall DA, Barrett DA, Chapman V. Analgesic effects of fatty acid amide hydrolase inhibition in a rat model of neuropathic pain. J Neurosci. 2006; 26:13318–13327. [PubMed: 17182782]
15. Ahn K, et al. Discovery and characterization of a highly selective FAAH inhibitor that reduces inflammatory pain. Chem Biol. 2009; 16:411–420. [PubMed: 19389627]
16. Cravatt BF, et al. Molecular characterization of an enzyme that degrades neuromodulatory fatty-acid amides. Nature. 1996; 384:83–87. [PubMed: 8900284]
17. Long JZ, et al. Selective blockade of 2-arachidonoylglycerol hydrolysis produces cannabinoid behavioral effects. Nat Chem Biol. 2009; 5:37–44. [PubMed: 19029917]
18. Kinsey SG, et al. Blockade of endocannabinoid-degrading enzymes attenuates neuropathic pain. J Pharmacol Exp Ther. 2009; 330:902–910. [PubMed: 19502530]
19. Long JZ, et al. Dual blockade of FAAH and MAGL identifies behavioral processes regulated by endocannabinoid crosstalk in vivo. Proc Natl Acad Sci U S A. 2009; 106:20270–20275. [PubMed: 19918051]
20. Pan B, et al. Blockade of 2-Arachidonoylglycerol Hydrolysis by Selective Monoacylglycerol Lipase Inhibitor 4-Nitrophenyl 4-(Dibenzo[d][1,3]dioxol-5-yl(hydroxy)methyl)piperidine-1-carboxylate (JZL184) Enhances Retrograde Endocannabinoid Signaling. The Journal of pharmacology and experimental therapeutics. 2009; 331:591–597. [PubMed: 19666749]
21. Straiker A, et al. Monoacylglycerol lipase limits the duration of endocannabinoid-mediated depolarization-induced suppression of excitation in autaptic hippocampal neurons. Mol Pharmacol. 2009; 76:1220–1227. [PubMed: 19767452]

Author Manuscript Author Manuscript Author Manuscript Author Manuscript


22. Wilson RI, Nicoll RA. Endocannabinoid signaling in the brain. Science. 2002; 296:678–682. [PubMed: 11976437]
23. Tanimura A, et al. The endocannabinoid 2-arachidonoylglycerol produced by diacylglycerol lipase alpha mediates retrograde suppression of synaptic transmission. Neuron. 65:320–327. [PubMed: 20159446]
24. Gao Y, et al. Loss of retrograde endocannabinoid signaling and reduced adult neurogenesis in diacylglycerol lipase knock-out mice. J Neurosci. 30:2017–2024. [PubMed: 20147530]
25. Haller J, et al. Interactions between environmental aversiveness and the anxiolytic effects of enhanced cannabinoid signaling by FAAH inhibition in rats. Psychopharmacology (Berl). 2009; 204:607–616. [PubMed: 19259645]
26. Liu Y, Patricelli MP, Cravatt BF. Activity-based protein profiling: The serine hydrolases. Proc. Natl. Acad. Sci. U.S.A. 1999; 96:14694–14699. [PubMed: 10611275]
27. Blankman JL, Simon GM, Cravatt BF. A Comprehensive Profile of Brain Enzymes that Hydrolyze the Endocannabinoid 2-Arachidonoylglycerol. Chem Biol. 2007; 14:1347–1356. [PubMed: 18096503]
28. Nomura DK, et al. Activation of the endocannabinoid system by organophosphorus nerve agents. Nat Chem Biol. 2008; 4:373–378. [PubMed: 18438404]
29. Long JZ, Nomura DK, Cravatt BF. Characterization of monoacylglycerol lipase inhibition reveals differences in central and peripheral endocannabinoid metabolism. Chem Biol. 2009; 16:744–753. [PubMed: 19635411]
30. Aceto MD, Scates SM, Lowe JA, Martin BR. Cannabinoid precipitated withdrawal by the selective cannabinoid receptor antagonist, SR 141716A. Eur J Pharmacol. 1995; 282:R1–R2. [PubMed: 7498260]
31. Falenski KW, et al. FAAH −/− Mice Display Differential Tolerance, Dependence and Cannabinoid Receptor Adaptation Following Δ9-Tetrahydrocannabinol and Anandamide Administration. Neuropsychopharmacology. 2010 **in press**.
32. Lichtman AH, Hawkins EG, Griffin G, Cravatt BF. Pharmacological activity of fatty acid amides is regulated, but not mediated, by fatty acid amide hydrolase in vivo. J. Pharmacol. Exp. Ther. 2002; 302:73–79. [PubMed: 12065702]
33. Wilson RI, Kunos G, Nicoll RA. Presynaptic specificity of endocannabinoid signaling in the hippocampus. Neuron. 2001; 31:453–462. [PubMed: 11516401]
34. Kreitzer AC, Regehr WG. Retrograde signaling by endocannabinoids. Curr Opin Neurobiol. 2002; 12:324–330. [PubMed: 12049940]
35. Monory K, et al. Genetic dissection of behavioural and autonomic effects of Delta(9)-tetrahydrocannabinol in mice. PLoS Biol. 2007; 5:e269. [PubMed: 17927447]
36. Lichtman AH, Martin BR. Cannabinoid tolerance and dependence. Handb Exp Pharmacol. 2005:691–717. [PubMed: 16596793]
37. Sim LJ, Hampson RE, Deadwyler SA, Childers SR. Effects of chronic treatment with delta9-tetrahydrocannabinol on cannabinoid-stimulated [35S]GTPgammaS autoradiography in rat brain. J Neurosci. 1996; 16:8057–8066. [PubMed: 8987831]
38. Romero J, et al. Effects of chronic exposure to delta9-tetrahydrocannabinol on cannabinoid receptor binding and mRNA levels in several rat brain regions. Brain Res Mol Brain Res. 1997; 46:100–108. [PubMed: 9191083]
39. Sun M, Lee CJ, Shin HS. Reduced nicotinic receptor function in sympathetic ganglia is responsible for the hypothermia in the acetylcholinesterase knockout mouse. J Physiol. 2007; 578:751–764. [PubMed: 17038428]
40. Lanoir J, Hilaire G, Seif I. Reduced density of functional 5-HT1A receptors in the brain, medulla and spinal cord of monoamine oxidase-A knockout mouse neonates. J Comp Neurol. 2006; 495:607–623. [PubMed: 16498683]
41. Luk T, et al. Identification of a potent and highly efficacious, yet slowly desensitizing CB1 cannabinoid receptor agonist. Br J Pharmacol. 2004; 142:495–500. [PubMed: 15148260]
42. Hillard CJ. Biochemistry and pharmacology of the endocannabinoids arachidonylethanolamide and 2-arachidonylglycerol. Prostaglandins Other Lipid Mediat. 2000; 61:3–18. [PubMed: 10785538]

Author Manuscript Author Manuscript Author Manuscript Author Manuscript

43. Sim-Selley LJ, Martin BR. Effect of chronic administration of R-(+)-[2,3-Dihydro-5-methyl-3-[(morpholinyl)methyl]pyrrolo[1,2,3-de]-1,4-b enzoxazinyl]-(1-naphthalenyl)methanone mesylate (WIN55,212-2) or delta(9)-tetrahydrocannabinol on cannabinoid receptor adaptation in mice. J Pharmacol Exp Ther. 2002; 303:36–44. [PubMed: 12235230]
44. Caille S, Alvarez-Jaimes L, Polis I, Stouffer DG, Parsons LH. Specific Alterations of Extracellular Endocannabinoid Levels in the Nucleus Accumbens by Ethanol, Heroin, and Cocaine Self-Administration. J. Neurosci. 2007; 27:3695–3702. [PubMed: 17409233]
45. Ohno-Shosaku T, Maejima T, Kano M. Endogenous cannabinoids mediate retrograde signals from depolarized postsynaptic neurons to presynaptic terminals. Neuron. 2001; 29:729–738. [PubMed: 11301031]
46. Fan F, Compton DR, Ward S, Melvin L, Martin BR. Development of cross-tolerance between delta 9-tetrahydrocannabinol, CP 55,940 and WIN 55,212. J Pharmacol Exp Ther. 1994; 271:1383–1390. [PubMed: 7996450]
47. Pertwee RG, Wickens AP. Enhancement by chlordiazepoxide of catalepsy induced in rats by intravenous or intrapallidal injections of enantiomeric cannabinoids. Neuropharmacology. 1991; 30:237–244. [PubMed: 1649415]
48. Lichtman AH, Cook SA, Martin BR. Investigation of brain sites mediating cannabinoid-induced antinociception in rats: evidence supporting periaqueductal gray involvement. J Pharmacol Exp Ther. 1996; 276:585–593. [PubMed: 8632325]
49. Thomas EA, et al. Clozapine increases apolipoprotein D expression in rodent brain: towards a mechanism for neuroleptic pharmacotherapy. J Neurochem. 2001; 76:789–796. [PubMed: 11158250]
50. Schlosburg JE, et al. Inhibitors of endocannabinoid-metabolizing enzymes reduce precipitated withdrawal responses in THC-dependent mice. AAPS J. 2009; 11:342–352. [PubMed: 19430909]

Author Manuscript Author Manuscript Author Manuscript Author Manuscript

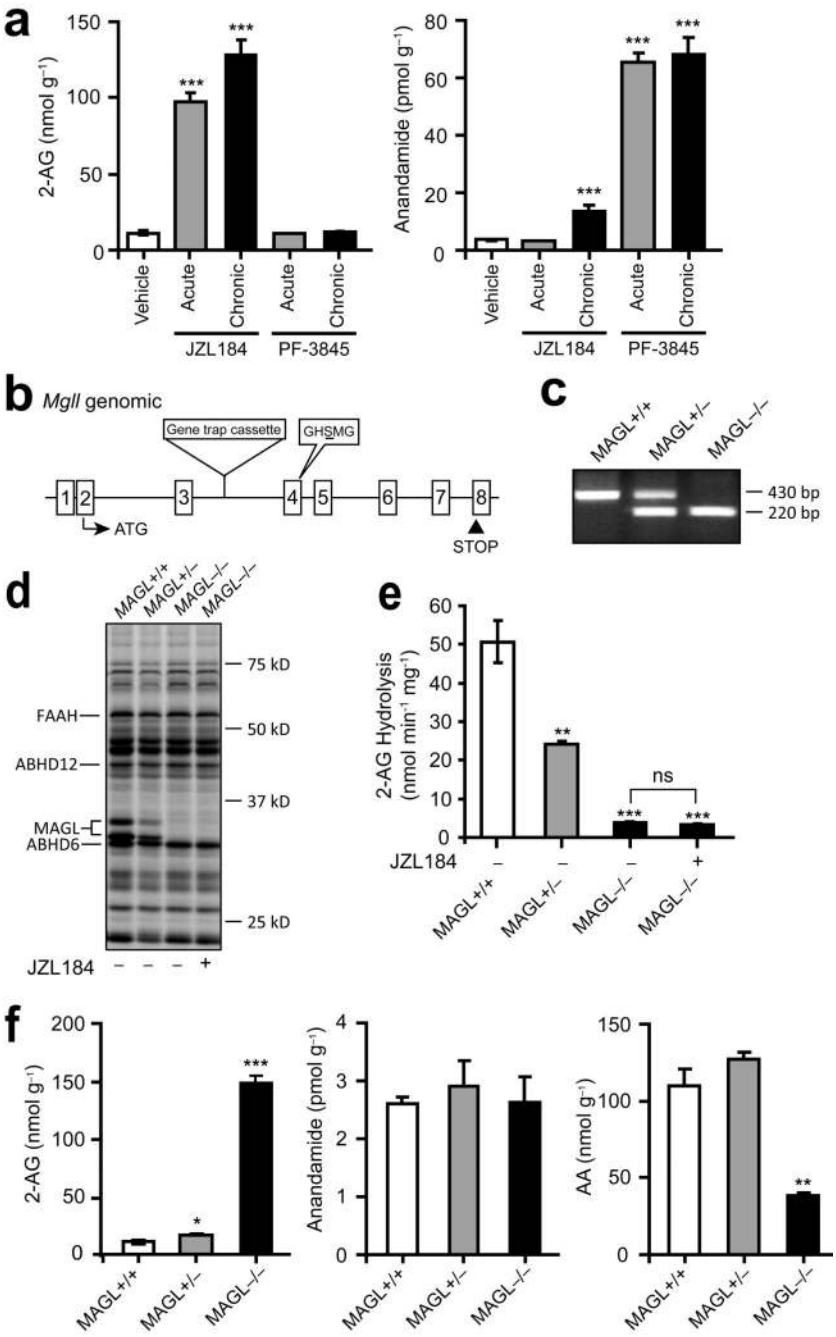


**Figure 1. Characterization of endocannabinoid metabolism in mice with chronic disruptions of MAGL or FAAH**

(**a**) Brain levels of 2-AG and anandamide in mice treated acutely or chronically with JZL184 (acute dosing regimen: 40 mg/kg, i.p., 2 h; chronic dosing regimen: six days, one dose per day, evaluated 2 h after final dose) or PF-3845 (acute dosing regimen: 10 mg/kg, i.p., 2 h; chronic dosing regime: six days, one dose per day, evaluated 2 h after final dose). n = 5–6 mice per group. (**b**) The genomic structure surrounding the integrated gene trap vector in *MAGL*$^{-/-}$ mice. The gene trap cassette inserted into the MAGL gene *Mgll* intron 3, upstream

Author Manuscript Author Manuscript Author Manuscript Author Manuscript

of the catalytic exon E4 (GHSMG sequence containing the catalytic serine nucleophile is shown). (**c**) PCR genotyping of *MAGL*$^{+/+}$, *MAGL*$^{+/-}$, and *MAGL*$^{-/-}$ mice from genomic tail DNA. The 430 bp band corresponds to the wild-type allele and the 220 bp band corresponds to the gene-trapped allele. (**d**) Activity-based protein profiling26,27 of brain membrane proteomes demonstrating the selective loss of active MAGL protein in *MAGL*$^{-/-}$ mice. (**e**) 2-AG hydrolytic activities of *MAGL*$^{+/+}$, *MAGL*$^{+/-}$, and *MAGL*$^{-/-}$ brain membrane proteomes; n = 4 per genotype. Note that treatment of the *MAGL*$^{-/-}$ brain proteome with JZL184 (5 μM) did not further decrease MAGL activity signals (**d**) or 2-AG hydrolysis (**e**), supporting the complete loss of MAGL in this sample. (**f**) Brain levels of 2-AG, anandamide, and arachidonic acid from *MAGL*$^{+/+}$, *MAGL*$^{+/-}$, and *MAGL*$^{-/-}$ mice; n = 4–6 mice per genotype. Data are presented as means ± s.e.m. *$p < 0.05$, **$p < 0.01$, ***$p < 0.001$ versus vehicle-treated (**a**) or wild-type littermate control mice (**e** and **f**) (Dunnett's post-hoc test).

Author Manuscript Author Manuscript Author Manuscript Author Manuscript

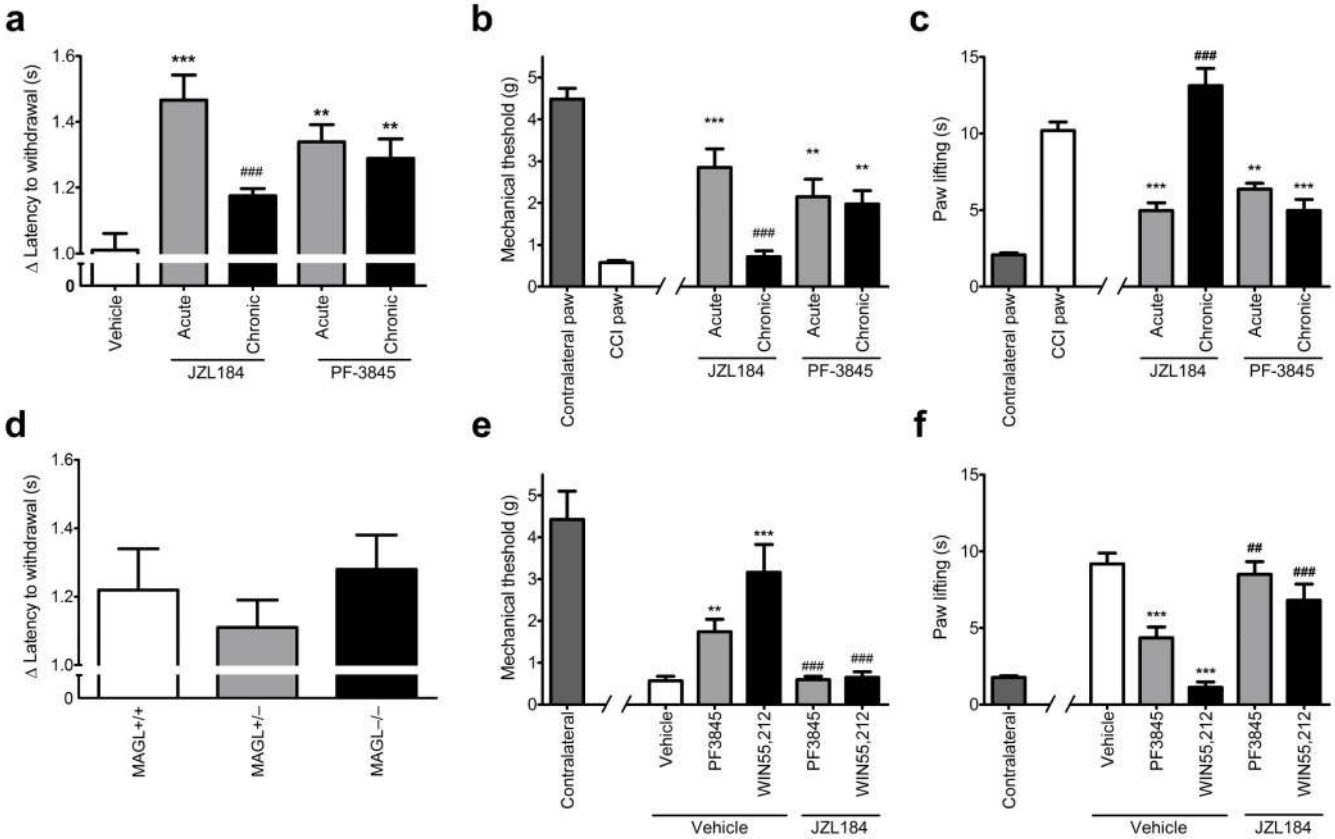


**Figure 2. Prolonged blockade of MAGL and FAAH causes differential analgesic tolerance**

(**a**) Acute treatment with JZL184 caused elevated withdrawal latencies in the tail immersion test for thermal nociception, while this hypoalgesic response was not observed following chronic treatment with JZL184 ($p = 0.33$). A similar magnitude hypoalgesic effect was observed in mice treated acutely with PF-3845, and this effect was maintained following chronic treatment with PF-3845. (**b, c**) Acute treatment with JZL184 or PF-3845 reduced mechanical (**b**) and cold (**c**) allodynia in nerve-injured mice. The anti-allodynic effects of PF-3845, but not JZL184, were maintained following chronic administration. (**d**) *MAGL*$^{+/+}$, *MAGL*$^{+/-}$, and *MAGL*$^{-/-}$ mice display similar tail withdrawal latencies. (**e, f**) Chronic JZL184 treatment causes cross-tolerance to the anti-allodynic effects of WIN55,212-2 and PF-3845. Data are presented as means ± s.e.m., with n = 6–8 per group in all studies. $^{*}p < 0.05$, $^{**}p < 0.01$, $^{***}p < 0.001$ versus vehicle-treated or wild-type littermate control mice (Dunnett's post-hoc test). $^{\#\#}p < 0.01$, $^{\#\#\#}p < 0.001$ versus respective acute drug treatment group (Bonferroni test).

Author Manuscript Author Manuscript Author Manuscript Author Manuscript

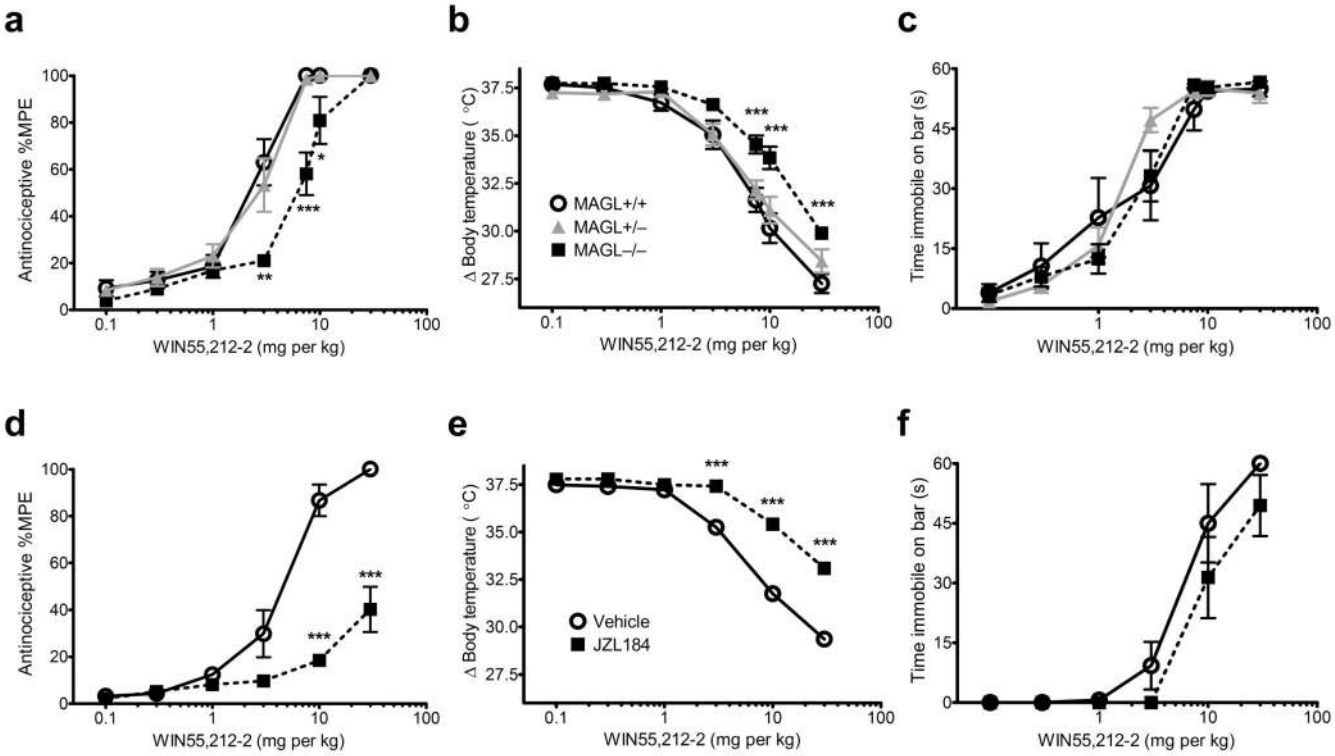


**Figure 3. Chronic disruption of MAGL produces behavioral cross-tolerance to a subset of the pharmacological effects of the cannabinoid receptor agonist WIN55,212-2**

(**a–c**) *MAGL*$^{-/-}$ mice displayed significant cross-tolerance to the antinociceptive (**a**) and hypothermic (**b**), but not the cataleptic (**c**) effects of WIN55,212-2. Similarly, chronic treatment with JZL184 caused significant cross-tolerance to the antinociceptive (**d**) and hypothermic (**e**), but not the cataleptic (**f**) effects of WIN55,212-2. Data are presented as means ± s.e.m. n = 7–8 per group. *$p < 0.05$, **$p < 0.01$, ***$p < 0.001$ versus vehicle-treated or wild-type littermate control mice (planned comparisons).

Author Manuscript Author Manuscript Author Manuscript Author Manuscript

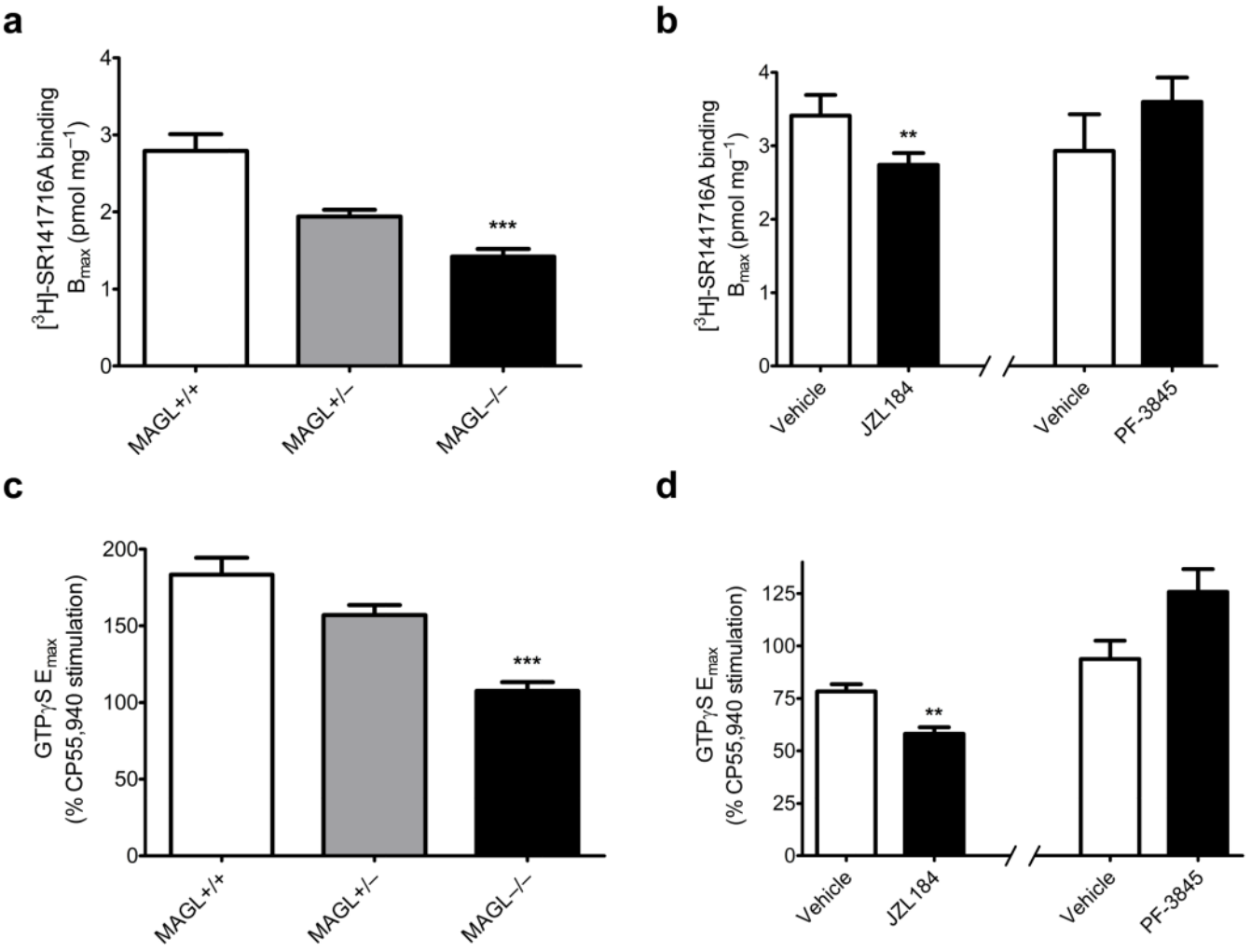


**Figure 4. Chronic disruption of MAGL produces $CB_1$ receptor down-regulation and desensitization in the mouse brain**

(**a**, **b**) Comparison of the membrane-specific $CB_1$ receptor binding by the antagonist [$^3$H]-SR141716A, as evaluated by the best-fit $B_{max}$ of binding curves from whole brain homogenates. *MAGL*$^{-/-}$ mice and mice treated chronically with JZL184, but not mice treated chronically with PF-3845, showed significant losses of $CB_1$ receptors. (**c**, **d**) CP55,940-stimulated [$^{35}$S]-GTPγS binding. *MAGL*$^{-/-}$ mice and mice treated chronically with JZL184, but not mice treated chronically with PF-3845, showed $CB_1$ receptor desensitization. Data are presented as means ± s.e.m. of nonlinear regression best-fit values of specific binding or sigmoidal dose-response curves. n = 4 tissue samples per group, run in separate experiments with each individual sample run in triplicate for GTPγS and duplicate for receptor binding. $^{**}p < 0.01$, $^{***}p < 0.001$ versus vehicle-treated or wild-type littermate control mice (determined by regression confidence intervals).

Author Manuscript Author Manuscript Author Manuscript Author Manuscript

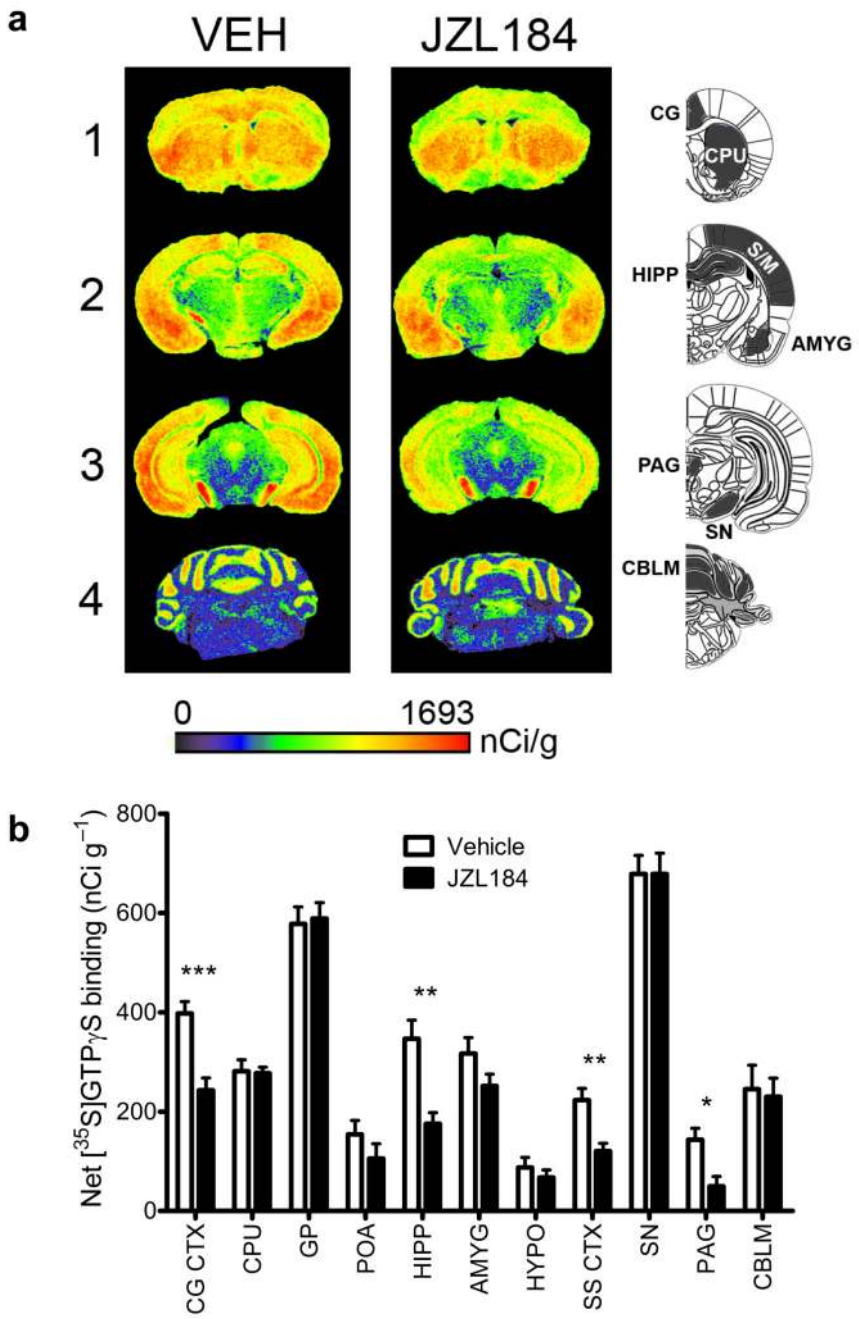


**Figure 5. Regional changes in cannabinoid agonist-stimulated [$^{35}$S]GTPγS binding following chronic disruption of MAGL**

(**a**) Representative autoradiograms showing CP55,940-stimulated [$^{35}$S] GTPγS binding in coronal brain sections following either chronic vehicle (left column) or JZL184 (right column) treatment. Pseudocolor images indicate levels of receptor-mediated G-protein activity and highlight significant decreases in $CB_1$ receptor activation in the cingulate cortex (CG, row 1), hippocampus (HIPP, row 2) and periaqueductal gray (PAG, row 3), while no differences are apparent in the caudate putamen (CPU, row 1) or cerebellum (CBLM, row

Author Manuscript Author Manuscript Author Manuscript Author Manuscript

4). (**b**) Densitometric analysis of CP55,940-stimulated [$^{35}$S]GTPγS binding in selected regions, including: cingulate cortex (CG CTX), caudate putamen (CPU), globus pallidus (GP), preoptic area of the hypothalamus (POA), hippocampus (HIPP), amygdala (AMYG), hypothalamus (HYPO), somatosensory cortex (SS CTX), substantia nigra (SN), periaqueductal gray (PAG), & cerebellum (CBLM). Data are presented as means ± s.e.m. n = 8 brains per group, run in triplicate slices for each targeted region. *$p < 0.05$, **$p < 0.01$, ***$p < 0.001$ versus vehicle treatment for specific region (Student's *t*-test).

Author Manuscript Author Manuscript Author Manuscript Author Manuscript

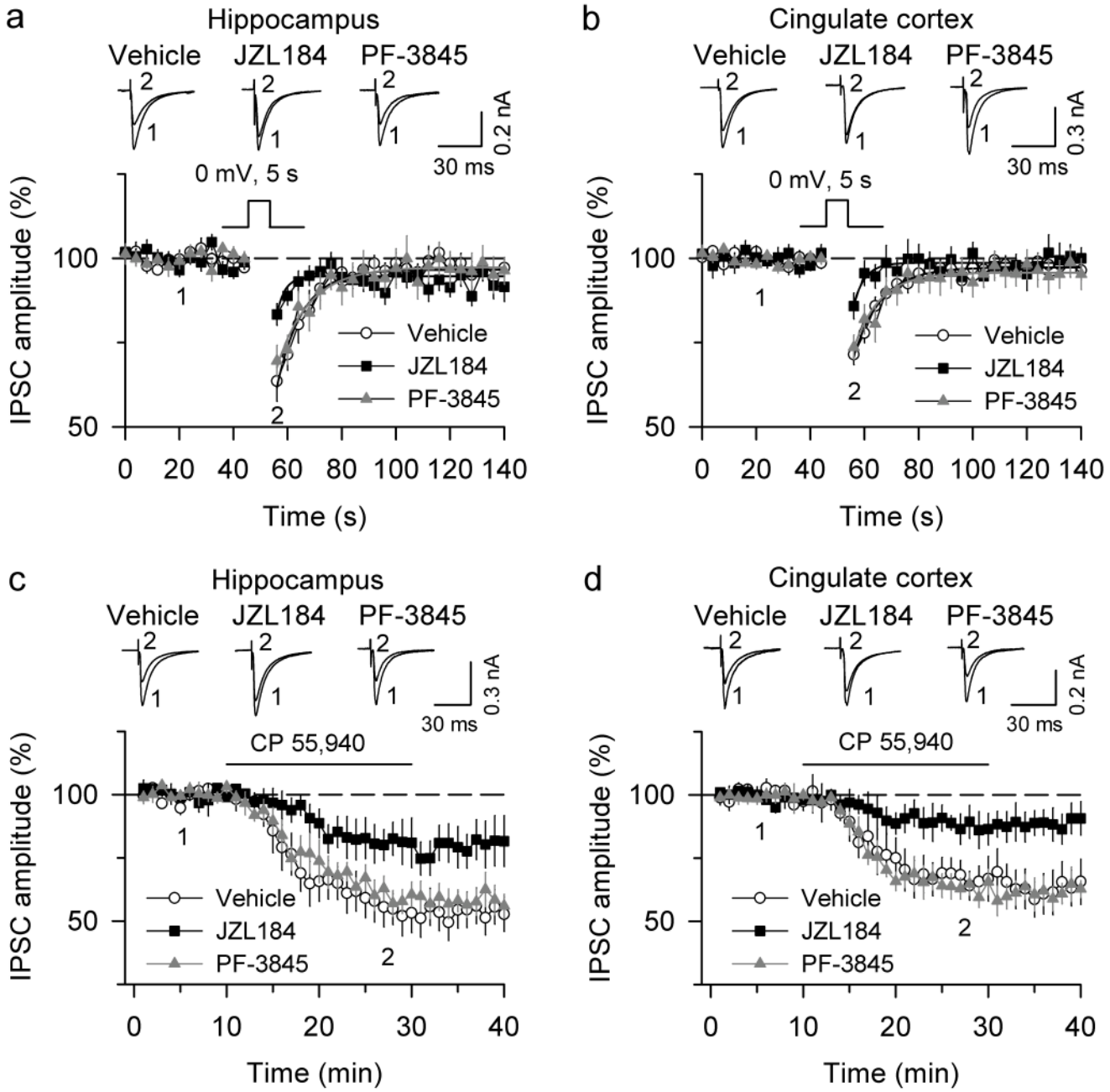


**Figure 6. Chronic disruption of MAGL impairs $CB_1$-dependent forms of synaptic plasticity**

(**a**, **b**) Chronic treatment with JZL184, but not PF-3845 attenuated DSI in hippocampal CA1 pyramidal neurons (**a**) and layer V pyramidal neurons of the cingulate cortex (**b**). For both magnitude and τ of DSI, $p < 0.01$ for JZL184- versus vehicle-treated groups. n = 11–15 mice per group. The lines superimposed are the single exponential fitting curves of the decay of DSI. (**c**, **d**) Bath application of the $CB_1$ agonist CP55,940 (3 μM) induced significantly less depression of IPSCs in the hippocampus (**c**) and cingulate cortex (**d**) from mice treated chronically with JZL184 compared to vehicle-treated control mice. $p < 0.05$ in both brain regions. Brain regions from mice treated chronically with PF-3845 did not differ

significantly from vehicle controls (n = 6–7 mice per group). Data are presented as means ± s.e.m.

Author Manuscript
Author Manuscript
Author Manuscript
Author Manuscript